# Exact Bounds on the Long Term Stability of Weakly Nonlinear Systems Applied to the Design of Large Storage Rings

Martin Berz and Georg Hoffstätter*

The motion in weakly nonlinear systems such as circular accelerators and storage rings can be described very well by high order Taylor maps representing the action on phase space. These transfer maps allow to obtain families of six-dimensional approximate invariants of motion. We present a method for obtaining a rigorous quantitative stability estimate which relies on bounding the deviation function describing fluctuations of the approximate invariants. To accomplish the task of maximizing the complicated functions involved, a very specialized interval maximizer had to be utilized. All calculations are performed within the COSY object-oriented language environment. In the paper, first, an overview of the problems occurring in weakly nonlinear systems in general and specifically in particle accelerators is presented. Then we discuss the computation of approximate invariants of motion in detail. Finally, the computer implementation and some results are described. Special emphasis is put on the interval optimization procedure.

# Точные границы долговременной устойчивости слабо нелинейных систем в применении к конструированию больших кольцевых накопителей

М. Берц, Г. Хоффштеттер

Движение в слабо нелинейных системах, таких как циклические ускорители и кольцевые накопители, хорошо описывается отображениями Тейлора

высоких порядков, представляющими действия в фазовом пространстве. Эти отображения переноса позволяют получать семейства приближенных шестимерных инвариантов движения. Представлен метод получения точной количественной оценки устойчивости через вычисление границ функций отклонения, описывающих флуктуации таких приближенных инвариантов. Чтобы справиться с задачей максимизации встречающихся при этом сложных функций, мы применили узко специализированный интервальный максимизатор. Все вычисления проводились в среде объектно-ориентированного языка COSY. В начале статьи представлен обзор проблем, связанных как со слабо нелинейными системами вообще, так и конкретно с ускорителями частиц. Затем подробно рассматривается вычисление приближенных инвариантов движения. В заключение описана реализация метода на ЭВМ и представлены некоторые результаты. Особое внимание уделено интервальной процедуре оптимизации.

# 1 Weakly nonlinear systems

In many ways, the study of the dynamics and in particular the global behavior of nonlinear systems is triggering a renaissance of classical mechanics. The concepts of chaos in nonlinear systems, albeit known per se for a long time, is generating fascination in circles far beyond the scientific community, and their study has become a fashion of remarkable proportion.

Nonlinear motions $\vec{x}(t)$ with initial value $\vec{x}_i$ are usually characterized by certain nonlinear differential equations

$$\frac{d}{dt}\vec{x} = \vec{f}(\vec{x}, t).$$

Of particular interest are the cases in which the function $\vec{f}$ is periodic in $t$ with period $T$; in these cases, the action of the system is often described in terms of the flow $\vec{M}$ which relates an initial condition $\vec{x}_i$ at time $t = 0$ to the final condition $\vec{x}_f$ at $t = T$:

$$\vec{x}_f = \vec{M}(\vec{x}_i).$$

In general it is not possible to determine the nonlinear map $\vec{M}$ in closed form, even if the function $\vec{f}$ is known in such a form, and for practical computations, $\vec{M}$ often has to be evaluated by numerical integration. In many important cases, however, the function $\vec{f}$ and with it the map $\vec{M}$ are actually dominated by linear parts and have only weak nonlinear perturbations.

In this case $\vec{f}$ and $\vec{M}$ can be described well by Taylor expansions. The use of high order automatic differentiation [5] as part of a differential algebraic approach has recently been shown [3, 4, 6] to allow the computation of the Taylor series of $\vec{M}$ to orders beyond ten in six or more variables. In its most elementary way, the method to compute the nonlinearities of $\vec{M}$ describing the flow of a certain differential equation is strikingly simple: viewing the numerical integrator as a method to evaluate the map $\vec{M}$ at any point, one just evaluates this functional dependence using automatic differentiation techniques.

In actuality, several refinements are needed to make the method practical. First of all, instead of automatic differentiation of the numerical integration process, which is very time consuming, one uses differential algebraic methods [4, 7] to evaluate the flow of short pieces, and obtains the flow for one period by composition of polynomials. In other cases, efficient scaling methods are used to obtain the maps for short sections [8].

## 2    The physics of beams

Perhaps currently the most important application of the above mentioned techniques for weakly nonlinear systems is the study of the motion in electromagnetic fields in the discipline of particle optics, which comprises the design of particle accelerators, particle spectrographs, and electron microscopes. In this case the motion is expressed in terms of three pairs of canonical variables which describe differences from a reference particle in horizontal ($x$) and vertical ($y$) positions and the relative energy deviation ($\delta_k$) as well as canonical conjugate momenta $a$, $b$, and $\tau$. The equations of motion take the form

$$
\begin{aligned}
x' &= a\,(1+hx)\frac{p_0}{p_z} \\
a' &= \left[(1+\delta_m)\frac{1+\eta}{1+\eta_0}\frac{p_0}{p_z}\frac{E_x}{\chi_{E_0}} - \frac{B_y}{\chi_{M_0}} + b\frac{p_0}{p_z}\frac{B_z}{\chi_{M_0}}\right](1+hx)(1+\delta_z) \;+\; h\frac{p_z}{p_0} \\
y' &= b\,(1+hx)\frac{p_0}{p_z} \\
b' &= \left[(1+\delta_m)\frac{1+\eta}{1+\eta_0}\frac{p_0}{p_z}\frac{E_y}{\chi_{E_0}} + \frac{B_x}{\chi_{M_0}} - a\frac{p_0}{p_z}\frac{B_z}{\chi_{M_0}}\right](1+hx)(1+\delta_z)
\end{aligned}
$$

$$\tau' = \frac{1-\eta_0}{2-\eta_0}\left[1 - (1+\delta_m)(1+hx)\frac{1+\eta}{1+\eta_0}\frac{p_0}{p_z}\right]$$

$$\delta'_k = 0$$

where $\vec{E}$ and $\vec{B}$ are the electric and magnetic fields, $\chi_m$ and $\chi_e$ are the magnetic and electric rigidities, $h$ is the momentary curvature of the reference orbit, and $\eta$ and $p_z/p_0$ have the form

$$\eta = \frac{K_0(1+\delta_k) - z_0 e(1+\delta_z)V(x,y,s)}{m_0 c^2(1+\delta_m)}$$

$$\frac{p_z}{p_0} = \sqrt{(1+\delta_m)^2\frac{\eta(2+\eta)}{\eta_0(2+\eta_0)} - a^2 - b^2}$$

where $m_o$, $z_0$, and $K_0$ describe mass, charge, and energy of the reference particle, the quantities $\delta_m$, $\delta_z$, and $\delta_k$ describe the relative deviations from these values, and $V$ is the electric potential.

In this case of particle optical motion, the linear coefficients of $\vec{M}$ describe properties connected to Gaussian optics, whereas the nonlinear terms describe aberrations. Historically, the computation of aberrations was a complicated problem, and very complex aberration formulas were derived for each element in a tedious way. In most cases, however, this could only be done to rather low orders around three.

Perhaps the most striking examples of beam physical systems where the above methods are used are the Superconducting Super Collider, the construction of which had begun near Dallas but has recently been terminated, as well as CERN's Large Hadron Collider, which is planned to be housed in the tunnel that is currently already used for the LEP electron positron collider. Table 1 gives an overview of some of the parameters of the SSC.

In the case of large scale accelerators, the main goal of beam simulation programs is to estimate the long term behavior of the particles; it is required that the machine has stable orbits for $100,000,000$ turns. Describing its transfer map $\vec{M}$ by a Taylor series of order around 10 gives a relative accuracy of about $10^{-12}$.

| Velocity of Protons | 99.99999987 % c |
|---|---|
| Energy per Proton | $2 \cdot 10^{13}$ eV |
| Total Energy of Protons | 800 MJ |
| Circumference | 83 km |
| Number of Revolutions | 100,000,000 |
| Number of Dipole Magnets | 7,700 |
| Number of Quadrupole Magnets | 1,800 |
| Estimated Cost | about $ 10 Billion |

Table 1: Some parameters of the Superconducting Super Collider

# 3  Normal form theory

The left picture in Figure 1 shows the motion for several turns in a typical accelerator, in this case the PSR II at Los Alamos National Laboratory. For each turn, the position $x$ as well as its canonical conjugate momentum $a$ is displayed. The irregular form of the band-like structure is due to nonlinear effects. The finite width of the band is a result of coupling to the other degree of freedom, the motion in $y$ direction. From the picture one can see that the particle positions are bounded for the number of turns shown. However, it is very difficult to estimate if the position is actually growing or shrinking and what would happen if the number of turns was increased. The right picture in Figure 1 shows the same motion in phase space after a nonlinear change of variables. The motion now has nearly circular shape, and it is much easier to make estimates about the long term stability. In fact, these methods provide the key to rigorous bounds on the stability of motion which we will discuss in the next section.

Normal form theory provides a nonlinear change of coordinates such that the motion in the new variables is rotationally invariant. Probably first introduced to the field in [9], normal form theory was first implemented to arbitrary order in a mixed differential algebraic—Lie algebraic framework [10] and recently simplified by casting it into a purely differential algebraic form [11]. In case the underlying motion is canonical, the transformation to normal form coordinates can be chosen canonical. This is the case in all Hamiltonian systems to which case we want to restrict the discussion for the remainder of the paper. The details of this normal form method can be found in [7, 11]. Here we only stress the steps pertaining to the desired stability estimates.
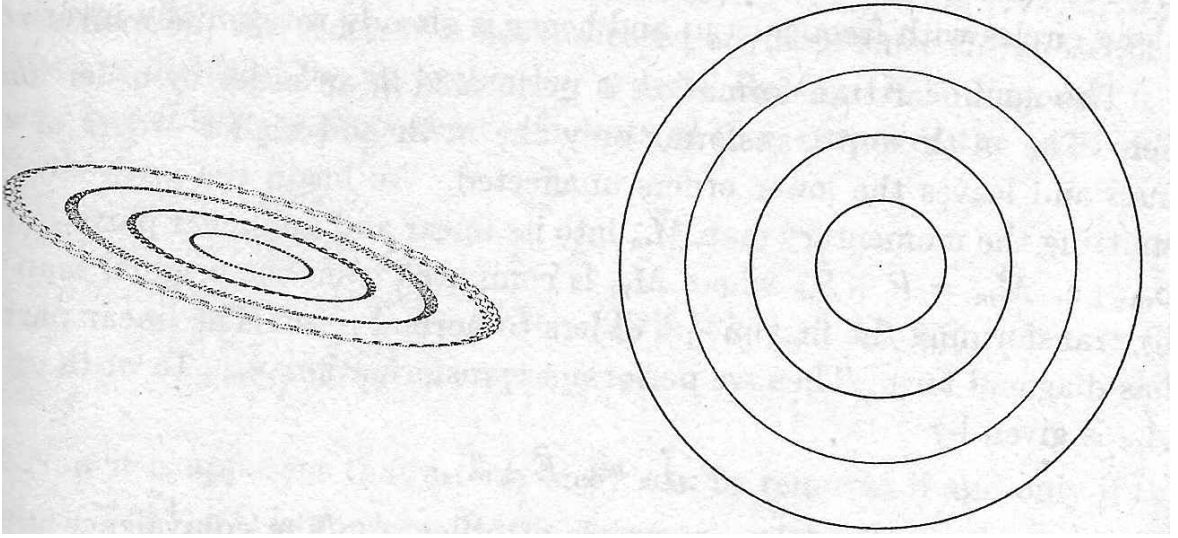
Figure 1: Phase Diagram for Motion in an Accelerator. The left picture shows the motion displayed in standard particle optical coordinates $x$ and $a$, and the right picture shows the same motion in normal form coordinates.

The coordinate transformation begins with a diagonalization of the linear part of the map. In the case of stable symplectic systems, the eigenvalues occur in complex conjugate pairs of unity modulus [12, 13]. When a vector is represented in the basis of eigenvectors, we denote its components by the variables $s_j^+$ and $s_j^-$ belonging to the eigenvectors $\vec{n}_j^+$ and $\vec{n}_j^-$ with eigenvalues $e^{+i\mu_j}$ and $e^{-i\mu_j}$, respectively. Complex conjugation of the eigenvector equation yields that $(\vec{n}_j^+)^*$ has the eigenvalue $e^{-i\mu_j}$ and is therefore proportional to $\vec{n}_j^-$. We choose $(\vec{n}_j^+)^* = \vec{n}_j^-$ and therefore $(s_j^+)^* = s_j^-$. To each variable pair $s_j^\pm$ we associate another pair $t_j^\pm$ of variables as follows:

$$
\begin{aligned}
t_j^+ &= (s_j^+ + s_j^-)/2 \\
t_j^- &= (s_j^+ - s_j^-)/2i.
\end{aligned}
\tag{1}
$$

In case of complex $s_j^\pm$, which corresponds to the stable case, the $t_j^\pm$ are just the real and imaginary parts of $s_j^+$ and thus are real. In the unstable case, $t_j^+$ is real and $t_j^-$ is imaginary. The $s_j^\pm$ can be expressed in terms of the $t_j^\pm$ as

$$
\begin{aligned}
s_j^+ &= t_j^+ + i\, t_j^- \\
s_j^- &= t_j^+ - i\, t_j^-.
\end{aligned}
\tag{2}
$$

In the normal form algorithm, it is advantageous to perform the manipulations in the $s_j^\pm$, while the results are most easily interpreted in the $t_j^\pm$. For example, the linear map expressed in the $t_j^\pm$ described the motion along circles with frequency $\mu_j$ and hence is already rotationally invariant.

The nonlinear transformation is performed in an order-by-order manner. The $m$-th step transforms only the $m$-th and higher orders of the map and leaves the lower orders unaffected. We begin the $m$-th step by splitting the momentary map $\vec{M}_m$ into its linear and nonlinear parts $\vec{R}$ and $\vec{S}_m$, i.e. $\vec{M}_m = \vec{R} + \vec{S}_m$ where $\vec{M}_m$ is computed from the original map $\vec{M}$ by transforming the first $m - 1$ orders to normal form. The linear part $\vec{R}$ has diagonal form. Then we perform a transformation $\vec{A}_m$. To $m$-th order $\vec{A}_m$ is given by

$$\vec{A}_m =_m \vec{E} + \vec{T}_m \tag{3}$$

where $\vec{T}_m$ possesses only monomials of order $m$. The equivalence up to order $m$ is indicated by $=_m$. Because the linear part of $\vec{A}_m$ is the unity map $\vec{E}$, $\vec{A}_m$ is invertible. We find that up to order $m$ we have

$$\vec{A}_m^{-1} =_m \vec{E} - \vec{T}_m. \tag{4}$$

Of course, the full inversion of $\vec{A}_m$ contains higher order terms, which will turn out to be one of the reasons why iteration is needed. It is also worth noting that in principle the higher order parts of $\vec{T}_m$ can be chosen freely, but there is an essentially unique transformation that is canonical. To study the effect of the transformation, we now infer up to order $m$:

$$
\begin{aligned}
\vec{A}_m \circ \vec{M}_m \circ \vec{A}_m^{-1} \;&=_m\; \left(\vec{E} + \vec{T}_m\right) \circ \left(\vec{R} + \vec{S}_m\right) \circ \left(\vec{E} - \vec{T}_m\right) \\
&=_m\; \left(\vec{E} + \vec{T}_m\right) \circ \left(\vec{R} + \vec{S}_m - \vec{R} \circ \vec{T}_m\right) \\
&=_m\; \vec{R} + \vec{S}_m + \left(\vec{T}_m \circ \vec{R} - \vec{R} \circ \vec{T}_m\right).
\end{aligned}
\tag{5}
$$

For the first step, we have used $\vec{S}_m \circ \left(\vec{E} - \vec{T}_m\right) =_m \vec{S}_m$ which holds because $\vec{S}_m$ is nonlinear and $\vec{T}_m$ is of order $m$. In the second step, we used $\vec{T}_m \circ \left(\vec{R} + \vec{S}_m - \vec{R} \circ \vec{T}_m\right) =_m \vec{T}_m \circ \vec{R}$ which holds because $\vec{T}_m$ is of exact order $m$ and everything in the second term is nonlinear except $\vec{R}$. This result can be used to simplify $\vec{S}_m$ by choosing the commutator $\vec{C}_m = \{\vec{T}_m, \vec{R}\} = \left(\vec{T}_m \circ \vec{R} - \vec{R} \circ \vec{T}_m\right)$ appropriately. Let $\left(T_{mj}^\pm \mid k_1^+, k_1^-, \ldots, k_n^+, k_n^-\right)$ be the Taylor expansion coefficient of $T_{mj}^\pm$ with respect to $(s_1^+)^{k_1^+}(s_1^-)^{k_1^-} \times \cdots \times (s_n^+)^{k_n^+}(s_n^-)^{k_n^-}$

in the $j$-th component pair of the map $\vec{T}_m$. So $T_{mj}^{\pm}$ is written as

$$T_{mj}^{\pm} = \sum (T_{mj}^{\pm}|k_1^+, k_1^-, \ldots, k_n^+, k_n^-) \cdot (s_1^+)^{k_1^+} (s_1^-)^{k_1^-} \times \cdots \times (s_n^+)^{k_n^+} (s_n^-)^{k_n^-}. \quad (6)$$

Similarly we identify the coefficients of $\vec{C}_m$ by $(C_{mj}^{\pm}|k_1^+, k_1^-, \ldots, k_n^+, k_n^-)$. From here on, the order $m$ is not indicated anymore since the subsequent steps are identical for all evaluation orders. Because $\vec{R}$ is diagonal, it is easily possible to express the coefficients of $\vec{C}$ in terms of the ones of $\vec{T}$. We obtain

$$\begin{aligned}
&(C_j^{\pm}|k_1, k_1^-, \ldots, k_n^+, k_n^-) \\
&= \left(e^{i\vec{\mu}\cdot(\vec{k}^+ - \vec{k}^-)} - e^{\pm i\mu_j}\right) \cdot (T_j^{\pm}|k_1^+, k_1^-, \ldots, k_n^+, k_n^-) \qquad (7) \\
&= C_j^{\pm}(\vec{k}^+, \vec{k}^-) \cdot (T_j^{\pm}|k_1^+, k_1^-, \ldots, k_n^+, k_n^-).
\end{aligned}$$

Now it is apparent that a term in $S_j^{\pm}$ can be removed if and only if the factor $C_j^{\pm}(\vec{k}^+, \vec{k}^-)$ is nonzero. If it is nonzero then the required term in $T_j^{\pm}$ is just the negative of the respective term in $S_j^{\pm}$ divided by $C_j^{\pm}(\vec{k}^+, \vec{k}^-)$. Therefore, the outcome of the whole normal form transformation depends upon the conditions under which the term $C_j^{\pm}(\vec{k}^+, \vec{k}^-)$ vanishes, which is the case if and only if the phases $\pm\mu_j$ and $\vec{\mu} \cdot (\vec{k}^+ - \vec{k}^-)$ agree modulo $2\pi$.

There are two cases when this can happen. The first case corresponds to $k_i^+ - k_i^- = \pm\delta_{ij}$, $\forall i \in \{1, \ldots, n\}$. Besides this unavoidable case, the phases can also agree modulo $2\pi$ if $\sum_i \mu_i n_i = 0 \mod 2\pi$ has nontrivial integer solutions $n_i$. The second case is called resonant; usually ring accelerators are designed to avoid this case. If Taylor maps up to order $n$ are analysed, the successive application of this order by order approach is described by

$$\vec{M}_1 = \vec{M}, \quad \vec{M}_{m+1} =_n \vec{A}_m \circ \vec{M}_m \circ \vec{A}_m^{-1}, \quad \vec{N} = \vec{M}_{n+1}. \quad (8)$$

$\vec{M}$ is the original map and $\vec{N}$ is called the corresponding normal form map. The definition of $\vec{A} = \vec{A}_n \circ \cdots \circ \vec{A}_1$ allows the short hand notation

$$\vec{N} = \vec{A} \circ \vec{M} \circ \vec{A}^{-1}. \quad (9)$$

Removing all possible terms by an appropriate choice of the $\vec{A}_m$ leaves only the terms associated with $k_i^+ - k_i^- = \pm\delta_{ij}$:

$$\begin{aligned}
N_j^+ &= \left(\sum (N_j^{\pm}|k_1^+, k_1^+, \ldots, k_j^+ + 1, k_j^+, \ldots)|s_1^+|^{2k_1^+} \ldots |s_n^+|^{2k_n^+} + e^{i\mu_j}\right)s_j^+, \\
N_j^- &= \left(\sum (N_j^{\pm}|k_1^+, k_1^+, \ldots, k_j^+, k_j^+ + 1, \ldots)|s_1^+|^{2k_1^+} \ldots |s_n^+|^{2k_n^+} + e^{-i\mu_j}\right)s_j^-.
\end{aligned}$$

where the fact that $s_i^+ = (s_i^-)^*$ was used. This shows that the dependence of the final coordinates $s_j^\pm|_f$ on the initial coordinates $s_j^\pm|_i$ is rotationally symmetric since it only depends on the amplitude but not on the phase in normal form space:

$$s_j^\pm|_f = f_j^\pm\big(|s_1^+|^2, \ldots, |s_n^+|^2\big) s_j^\pm|_i. \tag{10}$$

A detailed analysis reveals that $(f_j^+)^* = f_j^-$. Therefore, this transformation in general describes spirals in every $t_j^+$–$t_j^-$ subspace. Since for canonical motion volume in phase space is conserved, the motion has to be on circles and therefore $|f_j^\pm| = 1$. Thus in all $n$ projections to the two-dimensional subspaces given by the $t_j^\pm$, the motion is a rotation. The angle of every rotation can be a different function of the amplitudes $(t_j^+)^2 + (t_j^-)^2$ in the $n$ normal form subspaces in which the rotations occur. The invariants of motion are the radii of the rotations.

A complete transformation of the motion to circles can therefore only be possible if the motion is integrable. However, even if the motion were integrable, the presented approach involving Taylor maps to a specified order would only yield the Taylor expansions of the invariant radii to that order and would therefore recover approximate invariants. Nevertheless, the quality of the so generated invariants improves rapidly with evaluation order for weakly nonlinear systems.

As mentioned earlier, the left hand side of Figure 1 shows the motion in conventional coordinates. The right hand picture shows the same motion in normal form coordinates. The motion follows almost perfect circles. Both, the coupling from the other phase space coordinates and the nonlinear effects that lead to distortion have been removed.

# 4 Nekhoroshev-like stability estimates

Because of the clean appearance of motion in normal form coordinates, a rather detailed study of the dynamics is possible. For example, if the normal form motion would produce perfect circles, we know we have found an invariant of the system for each degree of freedom. Consider now the transformation of normal form circles to Cartesian variables. If this transformation is continuous, the resulting set is bounded and we can conclude that the motion is stable forever, and particles can never get lost.

Unfortunately, the motion in normal form coordinates does not follow perfect circles. Even if the system has invariants of motion, circular motion is approximated by a Taylor map. Another reason is the well known fact that many systems are nonintegrable, i.e. there is not an invariant for every degree of freedom. In such a case, the motion in normal form variables can not actually follow perfect circles even if no Taylor approximation was used, but must exhibit some very detailed fine structure deviating from perfectly circular motion.

If it were possible to design a system in such a way that the motion is indeed perfectly integrable, very small construction errors would entail a breakdown of this property. While the theory of Kolmogorov, Arnold, and Moser (see for example [14]) assures the survival of invariants under small perturbations in a rigorous mathematical way, the actual size of perturbations allowed within this theory is extremely small and certainly out of reach for all practical considerations.

It is worthwhile to study where this effect of breakdown of invariants comes from since the order-by-order procedure of the normal form algorithm attempts to obtain perfect circles to any given order. The key is that unfortunately, while the initial transfer map of the system may have a nicely and quickly converging Taylor series, this must not be true for the map describing the transformation to normal form coordinates and hence also not for the normal form motion. The reason is that, as (8) shows, there is an inherent problem of potentially small denominators of the form $\exp(i\vec{n}\cdot\vec{\mu}) - 1$ that can severly limit or even destroy convergence.

To study this property in some more detail, we show the invariant defects, i.e. the residual deviation from perfect invariance, for several cases. Figure 2 shows a plot of the invariant defects as a function of normal form radius and angle for a simple one-dimensional pendulum. In the case of this nonlinear motion, there is an invariant (the energy). Thus in principle, the normal form algorithm could converge. The left hand picture of Figure 2 shows the invariant defect for amplitudes of $1/10$ rad using a normal form map of order 16. In this case the scale is approximately $10^{-17}$, and all the errors are of a computational nature. In the right hand picture of Figure 2, the amplitude of the pendulum is increased to $1/2$ rad into a rather nonlinear regime. Again a normal form transformation map of order 16 was used. Now the scale of the invariant defects is $10^{-13}$, and some systematic effects due to the limited order become apparent.
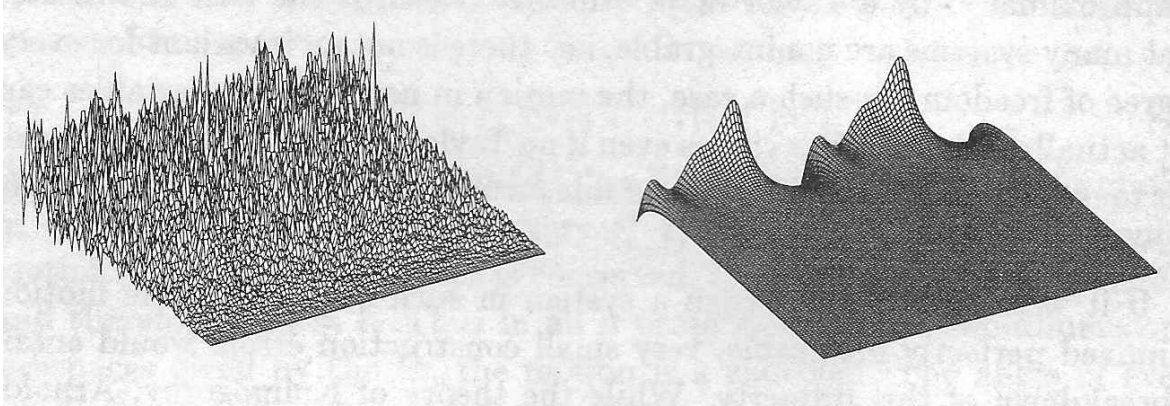
Figure 2: Deviations from invariance for a one-dimensional inharmonic pendulum as functions of normal form radius and angle. The oscillation amplitudes are 1/10 and 1/2 rad, respectively, and the scales on the errors are $10^{-17}$ and $3 \cdot 10^{-13}$, respectively. In both cases, the order of the normal form transformation map is 16.

In the next example we study the PSR II, a ring accelerator proposed by Los Alamos National Laboratory for which phase diagrams in conventional and normal form variables have been shown in Figure 1. In this case, an invariant does not have to exist a priori. It is rather likely that the motion is indeed nonintegrable, preventing convergence of the normal form map. Figure 3 again shows the invariant defect, i.e. the deviation from perfectly circular structure, in this case with a normal form transformation map of order 6. In the left hand picture, the defect is shown as a function of normal form radius and angle, and the increase with radius due to the limited convergence is clearly visible. The right hand picture shows the invariant defect as a function of the two normal form angles corresponding to horizontal and vertical motion. In both cases, the scale is about $10^{-6}$.

While the existence of invariant defects makes statements about general stability impossible, it still allows an estimate of stability for finite but long times. This has been recognized first by Nekhoroshev [1] and was later studied for several cases [15–19] by trying to fit models for approximate invariants to numerical data. Since in practice the invariant defects are very small, we can make estimates of how long a particle takes to traverse a certain region of normal form coordinate space for every of the $n$ subspaces in which the motion follows approximately circular shape. This method is illustrated in Figure 4 for one of those subspaces. Let us assume that the whole region of normal form coordinates up to the maximum radius $r_{\max}$
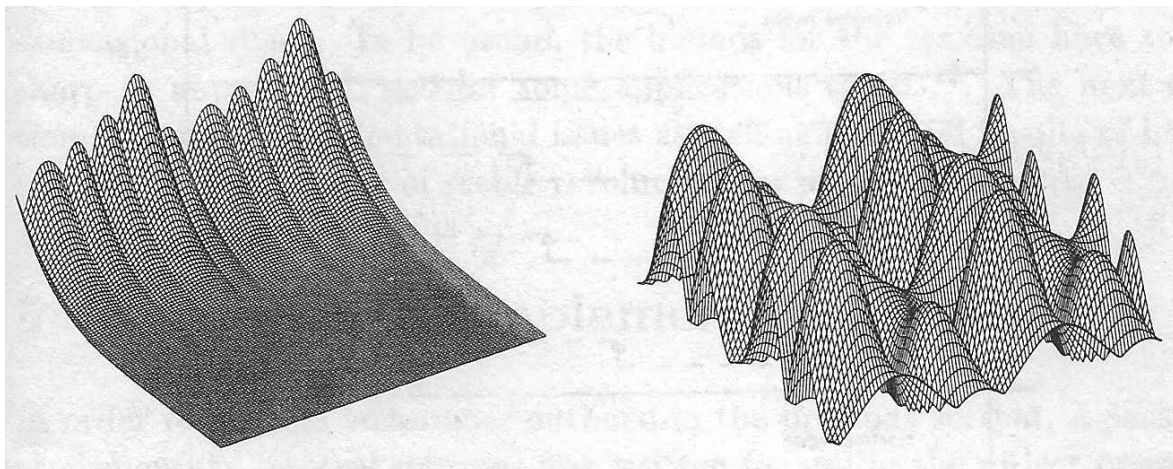
Figure 3: Deviations from invariance for the Los Alamos PSR II. The left hand picture shows the invariant defect as a function of horizontal normal form radius and angle. The right hand picture shows this defect as a function of the horizontal and vertical normal form angles.

corresponds to Cartesian coordinates within the area which the accelerator can accept in its beam pipes. Let us assume further that nowhere in the $r - \phi$ diagram is the invariant defect larger than $\Delta r$. If we launch particles within the normal form region below $r_{\min}$, then all these particles require at least

$$N = \frac{r_{\max} - r_{\min}}{\Delta r} \qquad (11)$$

turns before they reach $r_{\max}$. Considering the small size of $\Delta r$ in practical cases, this can often assure stability for a rather large number of turns.

In most cases, the invariant defects grow quickly with increasing values of $r$, as shown in Figures 2 and 3. Therefore, this estimate can be refined in the following rather obvious way. Suppose the region of $r$ values between $r_{\min}$ and $r_{\max}$ is subdivided in the following manner

$$r_{\min} = r_1 < r_2 < \cdots < r_l = r_{\max}. \qquad (12)$$

Let us assume that in each of these regions the maximum invariant defect is bounded by $\Delta r_i$. Then we can predict stability for

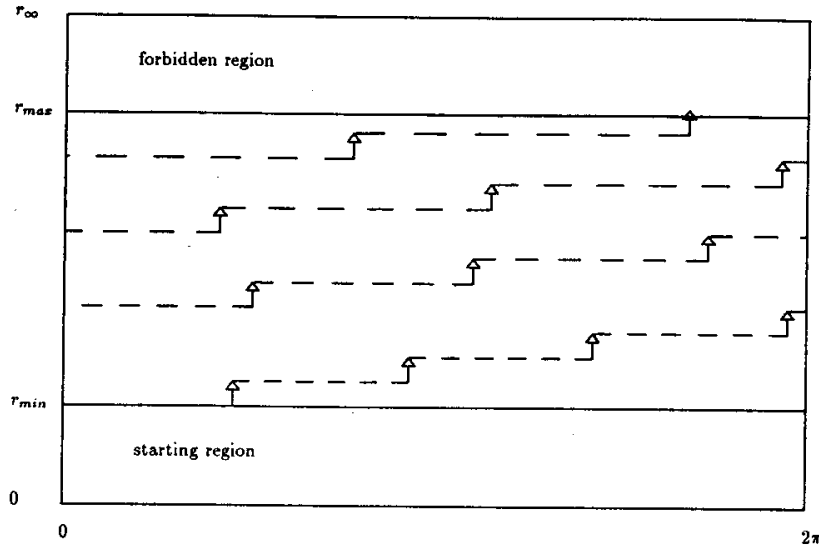$$N = \sum_{i=1}^{l-1} \frac{r_{i+1} - r_i}{\Delta r_i} \qquad (13)$$

Figure 4: Nekhoroshev-type estimate of the number of stable turns in a weakly nonlinear dynamical system. In any turn, the radius of the particle in normal form coordinates can grow by at most the invariant defect $\Delta r$. Thus it survives at least $N = (r_{\max} - r_{\min})/\Delta r$ turns.

turns. Since in practice, at least for the first values of $i$, $\Delta r_i$ can be substantially less than $\Delta r$, this lower bound can be much greater than $N$ in (11).

To determine the survival time of a particle, one can determine the corresponding numbers $N$ for every of the $n$ normal form subspaces and then take the smallest $N$ as a lower bound.

The appeal of the mathematically rigorous method outlined here hinges critically on the ability to determine rigorous bounds for the $\Delta r_i$ and its practical usefulness is directly connected to how sharp these bounds are. However, in practice these functions have a rather large number of local maxima, and a computation of their bounds requires quite some care. For every of the $l-1$ regions in phase space, we are faced with the task of finding $n$ bounds for the maxima $\Delta r^{(j)}$ of deviation functions:

$$\Delta r^{(j)} \geq \max \left[ r^{(j)}\big(\vec{M}(\vec{x})\big) - r^{(j)}(\vec{x}) \right] \tag{14}$$

where $r^{(j)}(\vec{x})$ is the normal form radius in the $j$-th normal form subspace of a particle at position $\vec{x}$. The regions in which the bounds for the maxima have to be found are the regions where $r^{(j)}(\vec{x}) \in [r_i^{(j)}, r_{i+1}^{(j)}]$. As illustrated

in Figures 2 and 3, those functions exhibit several local maxima in a six-dimensional space. To be useful, the bounds for the maxima have to be sharp to about $10^{-6}$, and for some applications to $10^{-12}$. The next section describes implementational issues as well as practical results of lower bounds on the number of stable revolutions for a variety of cases.

# 5 Questions of implementation

In order to use the techniques outlined in the previous section, a package of elementary interval routines was written for use in the object oriented language of COSY [20]. Since no direct access to hardware floating options is available, forced rounding is achieved by multiplication. In rather insensitive cases it is simply ignored.

A general difficulty with the problem at hand is that the objective function is rather complex. Furthermore, there are many large terms which cancel each other to finally give an approximate invariant such that a bound on very small fluctuations has to be found. This problem can be alleviated noticeably by rewriting the polynomial composition in such a way that some of the cancellations are actually performed by hand. It is possible to achieve this goal for the linear and the second order part of the polynomials. Since the contributions of the higher orders of the polynomials decrease rather quickly with the order, this eliminates a large source of blow-up.

However, even advanced methods of interval evaluation of polynomials, including rewriting of the involved polynomials as Horner factorizations up to fifth order and accurate bounding of the fifth order polynomials, does not reduce the blow-up sufficiently for the multidimensional functions of interest.

A satisfactory performance could only be achieved with the new data type of interval chains which is discussed in the following chapter. This specific method takes advantage of all the cancellations in the objective function.

# 6  Maximizing the deviation function with interval chains

The deviation function (14) is a polynomial with coefficients that cancel up to order $n$ if the map $\vec{M}$ and the normal form transformation $\vec{A}$ were computed to order $n-1$. The bothersome blow-up occurs because of this cancellation. If we found a method to bound only the contributions to a polynomial of order higher than $n$, we could evaluate the deviation function by bounding only the relevant orders. The cancellation of lower orders would not influence this result and thus all blow-up due to cancellations would be avoided. The concept of interval chains will achieve this goal.

An interval chain $I$ consists of a finite sequence of intervals $I_i$, $i \in \{0, \ldots, n+1\}$:

$$I = (I_0, I_1, I_2, \ldots, I_{n+1}) \tag{15}$$

where $I_i$ is called the $i$-th order of the interval chain. For interval chains, we define the elementary operations addition, scalar multiplication, and multiplication. The results of those operations are interval chains with the following elements:

$$
\begin{aligned}
(I + J)_i &= I_i + J_i, \ 0 \le i \le n+1, \\
(rI)_i &= rI_i, \ 0 \le i \le n+1, \ r \in \mathbb{R}, \\
(I \cdot J)_i &= \sum_{j=0}^{i} I_j J_{i-j}, \ 0 \le i \le n, \\
(I \cdot J)_{n+1} &= \sum_{i=0}^{n+1} (I_i \sum_{j=n+1-i}^{n+1} J_j).
\end{aligned}
\tag{16}
$$

For convenience of notation we denote the $i$-th order contribution of an $m$-th order polynomial $p$ by $p_i$. Then $p : \mathbb{R}^\nu \to \mathbb{R}$ can be written as $p : p(\vec{x}) = \sum_{i=0}^{m} p_i(\vec{x})$. For $i$ greater than $m$, $p_i$ is chosen to be zero. Call an interval chain $P(A^\nu) = (P_0, \ldots, P_{n+1})$ an interval chain (IC) evaluation of a polynomial $p$ of order $m$ on the interval box $A^\nu = A_1 \times \cdots \times A_\nu$ if $P_i \supseteq \{p_i(\vec{x}) | \vec{x} \in A^\nu\}$, $0 \le i \le n$ and $P_{n+1} \supseteq \{\sum_{i=n+1}^{m} p_i(\vec{x}) | \vec{x} \in A^\nu\}$. Thus $P_{n+1}$ bounds all contributions to the polynomial of order higher than $n$.

If $F(A^\nu)$ is an IC evaluation of a polynomial $f$ on $A^\nu$ and $G(A^\nu)$ is an IC evaluation of a polynomial $g$ on $A^\nu$, then $F(A^\nu) + G(A^\nu)$, $F(A^\nu) \cdot G(A^\nu)$, and $rF(A^\nu)$, $r \in \mathbb{R}$ are IC evaluations of $f + g$, $f \cdot g$, and $rf$ on $A^\nu$, respectively.

This can be seen as follows: Given the polynomials $f : f(\vec{x}) = \sum_{i=0}^{\alpha} f_i(\vec{x})$ and $g : g(\vec{x}) = \sum_{i=0}^{\beta} g_i(\vec{x})$, then by definition

$$
\begin{aligned}
F_i &\supseteq \{f_i(\vec{x})|\vec{x} \in A^\nu\}, & G_i &\supseteq \{g_i(\vec{x})|\vec{x} \in A^\nu\}, \ 0 \le i \le n, \\
F_{n+1} &\supseteq \{\textstyle\sum_{i=n+1}^{\alpha} f_i(\vec{x})|\vec{x} \in A^\nu\}, & G_{n+1} &\supseteq \{\textstyle\sum_{i=n+1}^{\beta} g_i(\vec{x})|\vec{x} \in A^\nu\}
\end{aligned}
\tag{17}
$$

from this we infer

$$
\begin{aligned}
\big(F(A^\nu) + G(A^\nu)\big)_i &= F_i + G_i \supseteq \{(f+g)_i(\vec{x})|\vec{x} \in A^\nu\}, \ 0 \le i \le n+1, \\
\big(rF(A^\nu)\big)_i &= rF_i \supseteq \{(rf)_i(\vec{x})|\vec{x} \in A^\nu\}, \ 0 \le i \le n+1, \\
\big(F(A^\nu) \cdot G(A^\nu)\big)_i &= \sum_{j=0}^{i} F_j G_{i-j} \supseteq \Big\{ \sum_{j=0}^{i} f_j(\vec{x}) g_{i-j}(\vec{x})|\vec{x} \in A^\nu \Big\} \\
&= \{(fg)_i(\vec{x})|\vec{x} \in A^\nu\}, \ 0 \le i \le n,
\end{aligned}
$$

$$
\begin{aligned}
\big(F(A^\nu) \cdot G(A^\nu)\big)_{n+1} &= \sum_{i=0}^{n+1} \Big( F_i \sum_{j=n+1-i}^{n+1} G_j \Big) \\
&= \sum_{i=0}^{n} \Big[ F_i \Big( \sum_{j=n+1-i}^{n} G_j + G_{n+1} \Big) \Big] + F_{n+1} \Big( \sum_{j=0}^{n} G_j + G_{n+1} \Big) \\
&\supseteq \Big[ \sum_{i=0}^{n} \Big[ f_i \Big( \sum_{j=n+1-i}^{n} g_j + \sum_{j=n+1}^{\beta} g_j \Big) \Big] + \Big( \sum_{i=n+1}^{\alpha} f_i \Big) \Big( \sum_{j=0}^{n} g_j + \sum_{j=n+1}^{\beta} g_j \Big) \Big] (A^\nu) \\
&= \Big[ \sum_{i=0}^{\alpha} \Big( f_i \sum_{j=\max(n+1-i,0)}^{\beta} g_i \Big) \Big] (A^\nu) \\
&= \Big[ \sum_{i=n+1}^{\alpha+\beta} \Big( \sum_{j=0}^{\beta} f_{i-j} g_j \Big) \Big] (A^\nu) = \Big\{ \sum_{i=n+1}^{\alpha+\beta} (fg)_i(\vec{x})|\vec{x} \in A^\nu \Big\}.
\end{aligned}
\tag{18}
$$

The expression in the fourth line from the bottom contains the expression in the next line since it is an interval evaluation of the function in the third line from the bottom.

Let now $\mathcal{A}$ be any algorithm based on addition, scalar multiplication, and multiplication that evaluates a polynomial $p$ at $\vec{x} = (x_1, \ldots, x_\nu)$. Then performing $\mathcal{A}$ on $\vec{I} = [(0, A_1, 0, \ldots, 0), \ldots, (0, A_\nu, 0, \ldots, 0)]$, a vector of interval chains, yields an IC evaluation of $p$ on $A^\nu$.

The following arguments prove this statement. For all $l \in \{1, \ldots, \nu\}$, $(0, A_l, 0, \ldots, 0)$ is an IC evaluation of the polynomial $i_l :\ i_l(\vec{x}) = x_l$ and $P(A^\nu)$ is the result of finitely many elementary operations which evaluate $p$ and therefore, using equations (6) and (18), we infer that $P(A^\nu)$ is an IC evaluation of $p$ on $A^\nu$.

Bearing this in mind, it is easy to see that for an IC evaluation $D(A^\nu)$ of the deviation function $d$ on $A^\nu$ it holds that $\{d(\vec{x}) | \vec{x} \in A^\nu\} \subseteq D_{n+1}$ since $d$ is known to have no orders lower than $n + 1$. In this approach cancellations up to order $n$ do not contribute and blow-up caused by such cancellations is avoided.

For practical purposes it proved essential to utilize a data type of vectors of interval chains. This is important since, as outlined in the previous section, the evaluation of the objective functions (14) requires three repeated evaluations of multidimensional polynomials. Because of symmetries, the coefficients usually exhibit sparseness, which suggests the determination of an optimal tree representation of the polynomials involved. Since the setup of this tree requires nonnegligible CPU time and is repeated for every evaluation of a multidimensional polynomial, it proved efficient to evaluate the polynomial with vectors of interval chains as arguments. In this way, the computation is facilitated by pushing many interval chains through the polynomial at once using the same tree representation.

But even with these simplifications, the resulting objective functions have a tendency to exhibit interval blow-up because of complexity, while the bounds of the function have to be determined rather tightly in order to guarantee large numbers of stable turns. Furthermore, the functions have a very large number of local maxima. All these effects make the exclusion of intervals rather difficult and not practically possible unless in the order of $10^4$ intervals per dimension are used. These large numbers make bookkeeping of intervals for later exclusion rather cumbersome if not impossible.

Because of this situation, the conventional methods based on disposing of intervals that can be excluded and halving of the remaining ones combined with occasional local optimization in real arithmetic [21, 22] are not directly applicable. For this reason, we are currently restricting ourselves to a mere rastering of the objective function with a large number of intervals of equal size. The results in the next section were obtained by choosing 630 intervals for the examples with one degree of freedom and 1000188 for the example with two degrees of freedom. Without the concept of interval chains a re-

alization af the described method was virtually impossible. For examples with two degrees of freedom approximately $10^{12}$ times more intervals would have been needed for similar results.

# 7  Results

Using the technique discussed in the previous sections, several nonlinear systems were studied using the interval chain rastering methods to provide upper bounds for the invariant defects. In order to get a feeling for the quality of these upper bounds, the numbers were compared with approximations for the maximal invariant defects obtained by a rather tight rastering in real arithmetic. Because of the large number of local maxima, this method proved to be the most robust noninterval way to estimate the absolute maxima of the functions involved. Lower bounds on the number of stable turns obtained by conventional intervals are given in the Tables 1 to 3 in order to illustrate the usefulness of interval chains. When conventional intervals were used, the deviation function was simplified as much as possible by accounting for cancellations up to second order analytically. The number of conventional intervals and the number of interval chains used in the bounding are equivalent. In all of the examples below, the choice of $r_{\max}$ is given, and $r_{\min}$ was chosen half as large.

| Order of Invariant | Interval Bounding (guaranteed) | Interval Chains (guaranteed) | Conventional Rastering (optimistic) |
|---|---|---|---|
| 3 | 11252 | 743,667 | 849,195 |
| 4 | 11252 | 743,667 | 849,195 |
| 5 | 11306 | 876,059,284 | 982,129,435 |
| 6 | 11306 | 876,059,284 | 982,129,435 |
| 7 | 11306 | 432,158,877,713 | 636,501,641,854 |
| 8 | 11306 | 432,158,877,713 | 636,501,641,854 |

Table 2: Predictions of the number of stable turns as a function of the order of the polynomials describing the normal form transformation for the physical pendulum $d^2/dt^2\phi + \sin(\phi) = 0$ for a time step of t=1 and an amplitude of 1/10 rad. Because of energy conservation, the map is known to be permanently stable for any amplitude.

As the first example to check the method, we used a one-dimensional physical pendulum. This is a good test case since energy conservation requires the nonlinear motion to be stable. Table 2 shows the results of the stability analysis for this case. As is to be expected, the number of stable turns predicted increases with the order and hence accuracy of the approximate invariants. While the approximate scanning method can take full advantage of this increased accuracy, the interval bounding method shows a saturation at 11306 turns. This asymptotic behavior is connected to the size of the intervals because of the unavoidable blow-up of intervals in the process of cancellation of large terms. The blow-up in third order dominates the calculation, causing the higher order improvements to not materialize. The method of interval chains takes care of all the cancellations and consequently the estimate is much better.

| Order of Invariant | Interval Bounding (guaranteed) | Interval Chains (guaranteed) | Conventional Rastering (optimistic) |
|---|---|---|---|
| 2 | 895 | 891 | 1,086 |
| 3 | 1736 | 9,926 | 11,450 |
| 4 | 1668 | 54,016 | 65,667 |
| 5 | 1674 | 678,725 | 809,612 |
| 6 | 1670 | 3,389,641 | 4,351,679 |
| 7 | 1671 | 42,640,927 | 52,474,387 |
| 8 | 1671 | 192,650,961 | 263,904,035 |

Table 3: Predictions of the number of stable turns for the Henon map at tune 0.13, strength parameter k = 1.1, and starting position of .01 as a function of the order of the polynomials in the normal form transformation.

As another example, we chose the Henon Map (see for example [14]), which is a standard test case for the analysis of nonlinear motion because it exhibits almost all of the phenomena encountered in Hamiltonian nonlinear dynamics. These include stable and unstable regions, chaotic motion, and periodic elliptic fixed points. The Henon map can even serve as a very simplistic model of an accelerator under the presence of sextupoles for chromaticity correction. The results of these calculations are shown in Table 3. Similar to the previous case, the number of predicted turns increases with order. In the case of interval bounding, the number of periodic turns shows

asymptotic behavior limited by blow-up. Again the superiority of strict bounding with interval chains is obvious.

| Order of Invariant | Interval Bounding (guaranteed) | Interval Chains (guaranteed) | Conventional Rastering (optimistic) |
|---|---|---|---|
| 3 | 179 | 16,137 | 38,385 |
| 4 | 179 | 18,197 | 38,857 |
| 5 | 173 | 309,356 | 560,309 |
| 6 | 173 | 347,312 | 613,135 |
| 7 | 171 | 925,531 | 2,184,998 |
| 8 | 171 | 1,004,387 | 2,248,621 |

Table 4: Predictions of the number of stable turns as a function of order of the approximate invariant for the Los Alamos PSR II storage ring for the motion in a phase space of 100 mm mrad.

In the final example, we study the Los Alamos PSR II already described above. The same data are shown as for the two previous examples. To limit the calculation time, the intervals used for the optimization were 5 times as wide as the intervals used for the previous two tables. While the guaranteed prediction of the interval chain method is about a factor of two lower than the optimistic estimate obtained from rastering, it is again far superior than the conventional interval method.

# References

[1] Nekhoroshev, N. N. *An exponential estimate of the time of stability of nearly integrable Hamiltonian systems I.* Uspekhi Mat. Nauk **32** (6). English translation: Russian Math. Surveys **1** (1977).

[2] Griewank, A. and Corliss, G. F. (eds) *"Automatic differentiation of algorithms".* SIAM, Philadelphia, Penn., 1991.

[3] Berz, M. *Differential algebraic description of beam dynamics to very high orders.* Particle Accelerators 24:109, 1989.

[4] Berz, M. *Arbitrary order description of arbitrary particle optical systems.* Nuclear Instruments and Methods A298:426, 1990.

[5] Berz, M. *Forward algorithms for high orders and many variables.* In preparation.

[6] Berz, M. *Automatic differentiation as nonarchimedean analysis.* In: "Computer Arithmetic and Enclosure Methods", Elsevier Science Publishers, Amsterdam, 1992, p. 439.

[7] Berz, M. *High-order computation and normal form analysis of repetitive systems.* In: Month, M. (ed.) "Physics of Particle Accelerators, AIP Conference Proceedings" 249:456, 1991.

[8] Hoffstätter, G. H. and Berz, M. *An efficient symplectic approximation for fringe-field maps.* AIP Conference Proceedings 297:467, 1993.

[9] Dragt, A. J. and Finn, J. M. *Normal form for mirror machine Hamiltonians.* Journal of Mathematical Physics 20(12):2649, 1979.

[10] Forest, E., Berz, M., and Irwin, J. *Normal form methods for complicated periodic systems: a complete solution using differential algebra and Lie operators.* Particle Accelerators 24:91, 1989.

[11] Berz, M. *Differential algebraic formulation of normal form theory.* In: Berz, M., Martin, S., and Ziegler, K. (eds) "IOP Conference Series" 131:77, 1992.

[12] Courant, E. D. and Snyder, H. S. *Theory of the alternating gradient synchrotron.* Annals of Physics 3:1, 1958.

[13] Berz, M. *Direct computation and correction of chromaticities and parameter tune shifts in circular accelerators.* In: "Proceedings XIII International Particle Accelerator Conference", Dubna, 1992.

[14] Lichtenberg, A. J. and Liebermann, M. A. *Regular and stochastic motion.* Springer, New York, 1983.

[15] Warnock, R. L., Ruth, R. D., Gabella, W., and Ecklund, K. *Methods of stability analysis in nonlinear mechanics.* SLAC–PUB 4846, 1989.

[16] Warnock, R. L. and Ruth, R. D. *Stability of orbits in nonlinear mechanics for finite but very long times.* In: Scandale, W. (ed.) "Nonlinear Problems in Future Accelerators", World Scientific, 1991.

[17] Warnock, R. L. and Ruth, R. D. *Long-term bounds on nonlinear Hamiltonian motion.* SLAC–PUB 5267, 1991.

[18] Turchetti, C. *Nekhoroshev stability estimates for symplectic maps and physical applications.* Springer Proceedings in Physics 47:223, 1990.

[19] Bazzani, A., Marmi, S., and Turchetti, G. *Nekhoroshev estimate for isochronous non resonant symplectic maps.* Preprint, University of Bologna.

[20] Berz, M. *COSY INFINITY Version 6 Reference Manual.* National Superconducting Cyclotron Laboratory, MSUCL–869, 1991.

[21] Ratz, D. *Private communication.*

[22] Knüppel, O. *Private communication.*

Department of Physics and Astronomy
National Superconducting
Cyclotron Laboratory
Michigan State University
East Lansing, MI 48824
USA